

RIGID-FOLDABLE CYLINDERS AND CELLS

Tomohiro TACHI and Koryo MIURA

Assistant Professor, The University of Tokyo, 3-8-1 Komaba, Meguro-Ku, Tokyo 153-8902, Japan, tachi@idea.c.u-tokyo.ac.jp
 Professor Emeritus, The University of Tokyo, Japan, miurak@gakushikai.jp

Editor's Note: Manuscript submitted 1 January 2012; revisions received 4 August and 16 October 2012; accepted 28 October. This paper is open for written discussion, which should be submitted to the IASS Secretariat no later than June 2013.

ABSTRACT

In this paper, we present newly explored families of rigid-foldable cylinders and the cellular structures constructed from these cylinders; the families include zonogon extrusion cells, bi-directionally flat-foldable cells, and a novel type of cells, i.e., woven cylinder cells. We show the geometry of such structures to demonstrate their validity, their parametric design method, and their kinetic behaviors. These types of structures exhibit continuous rigid-foldability as well as flat-foldability in one or two directions; further, they have different kinetic properties that are potentially applicable for different purposes. The newly proposed woven cylinder cellular structure is a bi-directionally flat-foldable one-DOF rigid-foldable structure and has a distinctive geometric property: structural stiffness against compression in one of three directions.

Keywords: origami, deployable structure, rigid-foldable structure, cellular structure, honeycomb.

1. INTRODUCTION

Collapsible cylindrical surfaces are useful in various designs, as such deployable structures can form a close-to-watertight surface that encloses a certain desired volume, and the surfaces can be compactly folded into a two-dimensional state. Several flat-foldable cylindrical deployable structures have been proposed thus far, e.g., by Hoberman [1], Guest and Pellegrino [2], Sogame and Furuya [3], Nojima [4], Kuribayashi et al.[5], and Wu et al. [6]. However, the deployment of these existing tubes rely on the in-plane elastic deformation or the traveling of hinges (Figure 1), and the structures cannot be applied to large-scale structures or robust and reusable mechanisms, including kinetic architecture, radiation shields for space structures, and bellows. This is because the structures do not have a geometrically valid continuous transformation path from one state to another.

In order to solve this geometric problem, we focused on rigid-foldable structures, which are polyhedral surfaces that realize continuous deployment mechanisms from one state to another if their facets and foldlines are substituted with rigid panels and hinges, respectively. One example of a rigid-foldable structure is a developable double corrugation surface or Miura-ori [7] (Figure 2).

Variations of such rigid-foldable structures that are homeomorphic to disks can be designed by only considering local (i.e., per vertex) fold angle conditions. However, in order to design cylindrical mechanisms, we need to solve global closure conditions, for which consideration of the symmetry is essential. Figure 3 shows a rigid-foldable disk that cannot form a valid rigid-foldable tube.

We have proposed several types of continuously foldable designs of cylindrical structures—thus, rigid-foldable cylinders—with a one-DOF mechanism [8][9]. We have found that some of these cylinders tessellate a 3D space without destroying continuous transformability. This leads to the concept of families of *rigid-foldable collapsible cellular structures*. Rigid-foldable cellular structures have not been extensively investigated from theoretical and geometrical viewpoints; however, individual examples such as a cellular structure by Hoberman [10] and an origami model by Yenn [11] are known.

In this paper, we review the geometry of these families of collapsible cylindrical and cellular structures. We show the validity of the structures, their generative design method, and their kinetic behaviors. We then propose a novel type of structures called *woven cylinder* structures. Woven

cylinder structures are bi-directional flat-foldable one-DOF rigid-foldable structures similar to other rigid-foldable cells. In addition, they have the distinctive geometric property of being stiff against compression in one of three directions.

In Section 2, we show the basic transformable tube structure and then generalize it for the zonogon extrusion type (Section 3, [8]) and bi-directionally flat-foldable types (Section 4, [9,12]). In Section 5, we show the novel cellular structure type constructed from the basic tube structure. In Section 6, we compare the kinetic and static behaviors of these structures and propose possible applications of the cylindrical and cellular structures.

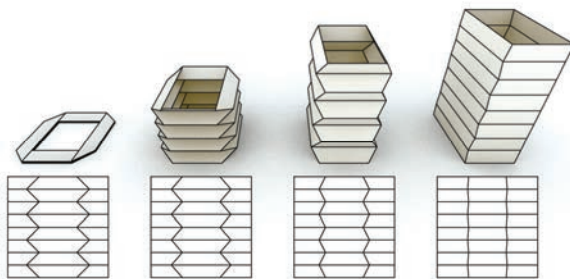


Figure 1. Conventional bellows. Note that the creases traverse the surface as the structure folds.

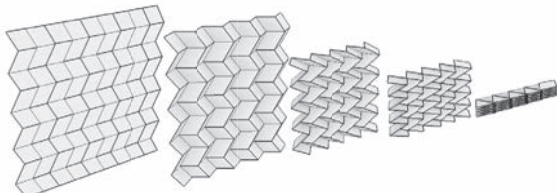


Figure 2. Miura-ori is a one-DOF rigid-folding mechanism homeomorphic to a disk.

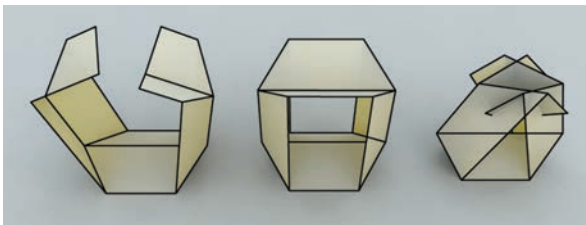


Figure 3. A tube constructed from a rigid-foldable disk does not generally transform.

2. BASIC FORM

2.1 Construction

In order to construct valid variations of rigid-foldable cylinders, we start from a very simple rigid-foldable tubular module: a polyhedron with

eight parallelogram panels. The module is constructed by mirroring a single Miura-ori vertex with four parallelograms with respect to the zx -plane (Figure 2). Observe the boundary curves of the Miura-ori vertex (shown in dotted lines). Since the vertex is constructed from congruent parallelograms, the curves are planar and are parallel to each other throughout the transformation.

The end loops of this module (shown in thick lines) are always each planar and parallel to each other. Therefore, the module can be packed in the z direction to form a tube, as shown in Figure 5.

Furthermore, the unit tube can be assembled to tessellate 3D space without gaps because of its translational symmetry. This symmetric behavior is compatible with the folding motion; thus, the tessellated structure can also validly transform.

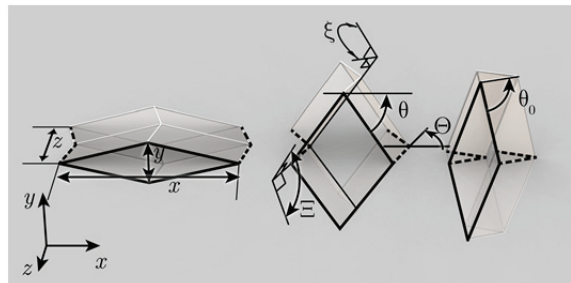


Figure 4. Tubular module.

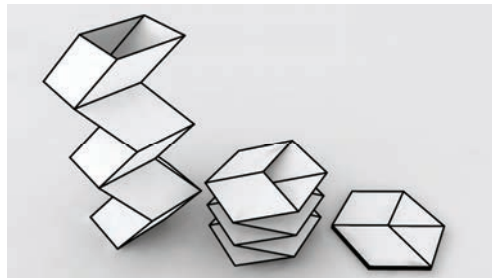


Figure 5. Constructed tube.

2.2 Kinetic Behavior

As shown in Figure 4, we denote the dihedral angles between adjacent parallelograms by ξ and Ξ . We denote the half of the angles between adjacent edges by θ and Θ , where θ and Θ vary from 0 to θ_0 . Here, θ_0 is an intrinsic parameter defining the shape of the parallelogram; thus, it is constant with respect to the folding motion. These four angle parameters ξ , Ξ , θ , and Θ are related by the following three equations to form a one-DOF mechanism.

$$\begin{cases} \tan \theta = \tan \theta_0 \cos \frac{\xi}{2}, \\ \sin \Theta = \sin \theta_0 \sin \frac{\xi}{2}, \\ \sin \theta = \sin \theta_0 \sin \frac{\Xi}{2} \end{cases} \quad (1)$$

Therefore, the dimensions of the module can be written as the functions of a single angle parameter ξ .

$$\begin{cases} x = x_0 \cos \theta = \frac{x_0}{\sqrt{1 + \tan^2 \theta_0 \cos^2 \frac{\xi}{2}}}, \\ y = y_0 \frac{\sin \theta}{\sin \theta_0} = \frac{y_0 \frac{1}{\cos \theta_0} \cos \frac{\xi}{2}}{\sqrt{1 + \tan^2 \theta_0 \cos^2 \frac{\xi}{2}}}, \\ z = z_0 \sin \frac{\xi}{2} \end{cases} \quad (2)$$

Equation 2 shows that the dimensions in the x , y , and z directions are monotonous functions with respect to the change in the folding angle. Further, the structure is bi-directionally flat-foldable in both the y and z directions. The folding motion in the case $\theta_0 = 2 \arctan(\sqrt{2}/2)$ is shown in Figure 6.

Since the tubes are packed without rotation, the kinetic behavior of the cellular structure is proportional to the original module with eight parallelograms and thus also satisfies Equation 2.

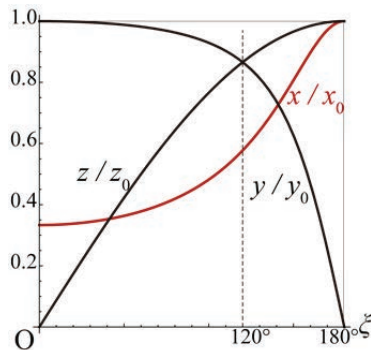


Figure 6. Folding motion of the eight-parallelogram module of $\theta_0 = 2 \arctan(\sqrt{2}/2)$.

3. ZONOGON EXTRUSION TYPE

3.1 Geometric Construction

A basic cylinder with eight parallelograms is generated by a zigzagged extrusion of a section parallelogram (Figure 5). The section curve can be generalized to an arbitrary zonogon while maintaining the rigid-foldability. The construction procedure (Figure 7) is as follows.

1. Draw an arbitrary closed polyline with two-fold rotational symmetry, i.e., a zonogon, on the section plane (the xy plane). We call this zonogon a “section zonogon.”
2. Make an arbitrary vector on the zx plane, which forms an angle of $\xi_0/2 < 90^\circ$ with the section plane. We call this vector the “extrusion vector” and denote it by $\mathbf{l}_0 = (\ell \cos \xi_0/2, 0, -\ell \sin \xi_0/2)$, where the vector has a length of ℓ .
3. Extrude the section zonogon by the extrusion vector to form a closed parallelogram strip.
4. Construct a zigzagged cylinder by sequentially mirroring the strip by plane, including the translated section zonogon.

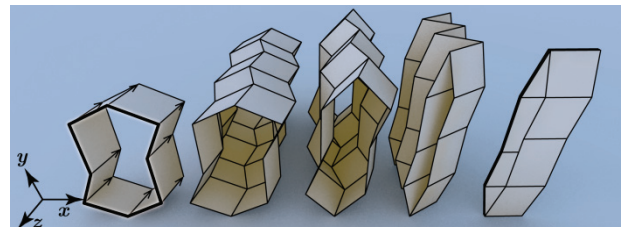


Figure 7. Zigzagged extrusion of a zonogon produces a valid rigid-foldable cylinder.

3.2 Validity

The validity of the transformation can be confirmed as follows. We pick up the extrusion of the half of the section zonogon along the extrusion vector forming an open parallelogram strip.

- (1) When we fold the strip along its edges, it is ensured that the edges, i.e., the extruded vertices, remain parallel after folding. We represent these parallel edges by a rotated extrusion vector $\mathbf{l} = (\ell \cos \xi/2, 0, -\ell \sin \xi/2)$.
- (2) Since adjacent strips are mirror images of each other, the section zonogon continues to lie on the section plane throughout the transformation process.

Constraints (1) and (2) imply that each facet

determines its orientation from the extruded vector and its original orientation. This results in a half cylinder with a one-DOF mechanism, whose two ends are translationally symmetric to each other. The other half strip is folded in the same manner. Since its deformed section zonogon is congruent to that of the first half, the two strips are compatible with each other and form a single rigid-foldable tube.

3.3 Kinetic Behavior

Assume that a segment of the section zonogon forms angle θ ($-90^\circ < \theta \leq 90^\circ$) with the x axis. This is represented as a vector $\mathbf{r} = (r\cos\theta, r\sin\theta, 0)$, where r is the length of the segment (Figure 6). The vector \mathbf{r} is rotated such that the angle between the edge and the extrusion vector is constant. Therefore, we obtain the constraint $\mathbf{l} \cdot \mathbf{r} = \text{constant}$, which results in the following relation (Figure 8):

$$\cos\theta = \frac{\cos\frac{\xi_0}{2}}{\cos\frac{\xi}{2}} \cos\theta_0, \quad (3)$$

where $\theta_0 = \theta|_{\xi=\xi_0}$. The valid sign of θ is chosen so that a continuous motion is produced, i.e., $\text{sign } \theta = \text{sign } \theta_0$ if $\theta_0 \neq 0$. If $\theta_0 = 0$, the mechanism has a singularity at $\theta = \theta_0 = 0$ so that both orientations are allowed.

The folding motion of a facet is represented as follows.

$$\begin{aligned} x &= \frac{\cos\frac{\xi_0}{2}}{\cos\frac{\xi}{2}} x_0, \\ y &= r \sqrt{1 - \frac{\cos^2\frac{\xi_0}{2}}{\cos^2\frac{\xi}{2}} \cos^2\theta_0}, \\ z &= z_0 \sin\frac{\xi}{2}. \end{aligned} \quad (4)$$

Here, the domain of ξ is given by $\cos\frac{\xi}{2} \geq \cos\frac{\xi_0}{2} \cos\theta_0$, where equality holds when $y = 0$. For a global structure with multiple edges of different θ_0 , the shallowest edge, i.e., the edge with the highest value of $\cos\theta_0$, limits the domain of global variable ξ . Therefore, the structure does not generally fold

flat in the y direction. On the other hand, the structure always collapses in the z direction when $\xi = 0$. Although there is a difference in the details depending on the shape of the zonogon, as a whole, the dimensions in the x , y , and z directions are monotonous functions with respect to the change in the folding angle. Figure 9 shows the folding motion for a hexagonal cylinder as an example.

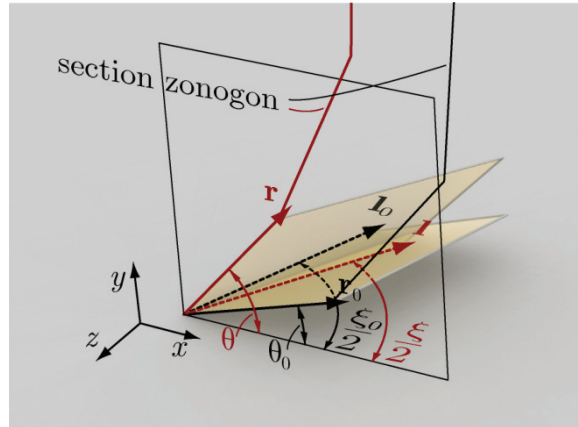


Figure 8. Folding motion of each facet. Note that vector r is determined independent of connectivity.

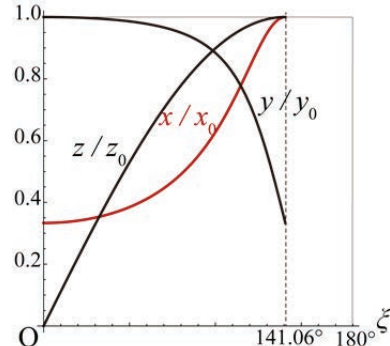


Figure 9. Folding motion of an example cylinder from a hexagonal section polygon. Note that the structure is only flat-foldable in the z direction.

3.4 Cellular Structures

The fact that the orientation of each facet is determined independent of adjacent faces implies that if multiple cylinders are constructed from zonogons sharing a vertex and edges, then these cylinders transform without producing any gaps. Hence, a planar tessellation of zonogons can be used as the section to produce a rigid-foldable cellular structure. The tessellation does not necessarily have periodic symmetry. Figures 10 and 11 show examples of a cellular structure using Penrose tiling and a multi-layered structure following a given curve, respectively.

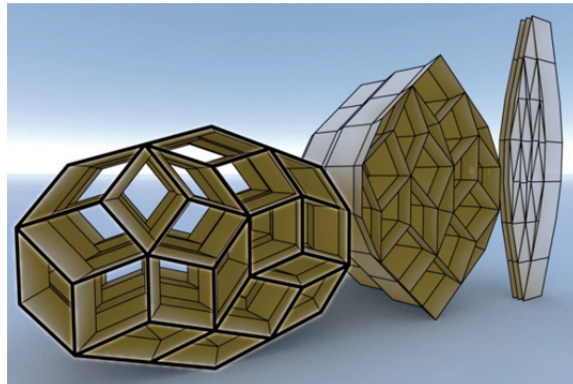


Figure 10. Example of a rigid-foldable cellular structure constructed from a zonogon tiling (Penrose tiling).

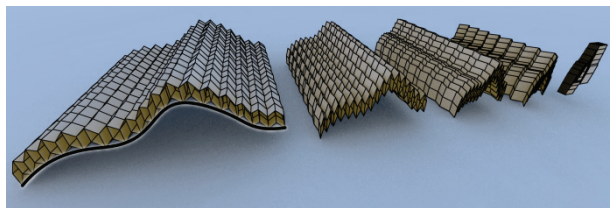


Figure 11. Example of a rigid-foldable cellular structure constructed from a given curve

4. BI-DIRECTIONALLY FLAT-FOLDABLE TYPE

4.1 Construction

The basic tube is not a single developable surface but a compound of two developable sheets sharing congruent boundary curves. By carefully constructing such a bi-directionally flat-foldable cylinder, we can construct valid mechanisms. The following is an overview of the construction steps.

1. Construct a one-DOF mechanism based on a quadrilateral array, such that each of two pairs of ends (in the z and x directions) comprises translationally symmetric boundary curves in any folded state.
2. Construct a structure compatible with the result of step 1. so that both surfaces share the same boundary curves, then connect the two surfaces.
3. Trim the doubly covered surface (if it exists) to construct a singly covered valid cylinder.

4.2 TMP (Tachi-Miura Polyhedron)

We show an example design of a bi-directionally flat-foldable cylindrical structure. First, consider a modular rectangle composed of nine facets with four identical Miura-ori vertices as its crease pattern,

as denoted in Figure 12. We can easily generalize the rectangular module so that it has 5, 7, or $2n + 1$ columns by repeating the same tile structure.

This surface transforms while preserving the parallelism of the fold lines and the planarity and congruency of the end polylines. This enables us to set a local coordinate that works throughout the transformation. As shown in Figure 13, we can extract two pairs of planes that do not rotate by folding, specifically, the 3- and 0-planes parallel to the xy plane and the A- and D-planes parallel to the yz plane.

Then, we produce a mirror image of the module with respect to its D-plane. This connects two units to form a half cylinder. The boundary polygons at the A-plane and its mirror A' plane are translationally symmetric to each other and have a common axis of 180° rotational symmetry (A-axis) (Figure 14).

We can then construct the other compatible half cylinder by rotating the original half cylinder by 180° around the A-axis. This forms a valid cylinder of a partially doubly covered surface. If we trim the doubly covered part, we obtain a star-like rigid-foldable cylinder (Figure 15). We can then extend the cylinder in the z direction. Figure 16 shows the crease pattern of two sheets comprising the cylinder for $\alpha = 45^\circ$.

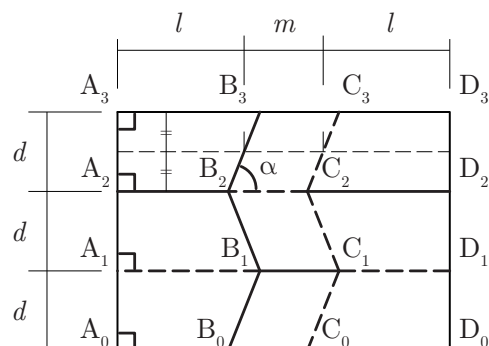


Figure 12. Crease pattern of nine-facet module.

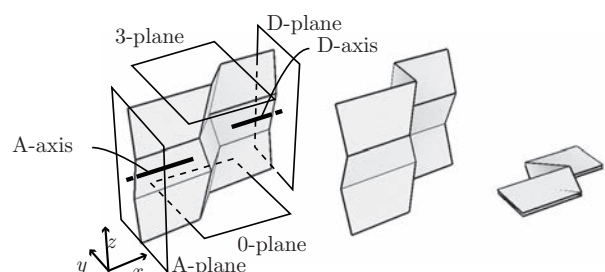


Figure 13. Coordinate system and planes.

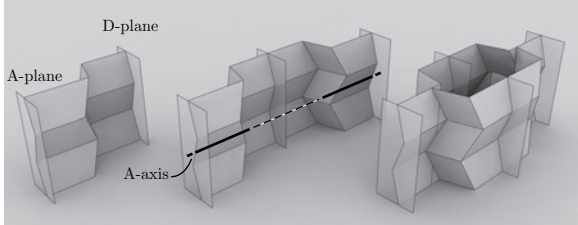


Figure 14. Symmetry operation to construct a cylinder by constructing the modules.

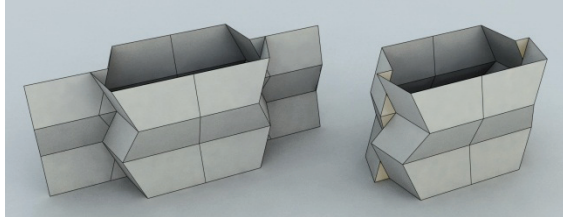


Figure 15. Trimming out the singly covered star-shaped polyhedron.

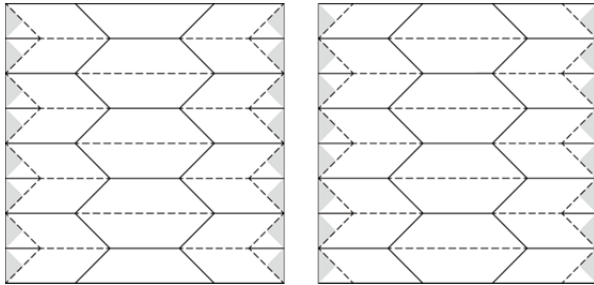


Figure 16. Crease pattern of the cylinder ($\alpha = 45^\circ$).

4.3 Kinetic Behavior

Patterns with different α produce different folding motions. Figures 17 and 18 show the transformation of cylinders when $\alpha = 45^\circ$ and 54° , respectively, with the common parameters $l = 1, m = 2, d = 1, N = 9$. For any parameter, the x and z dimensions are monotonous functions of the folding angle, such as for a basic tube. However, the y dimension holds a maximum value at $\cos \frac{\xi}{2} = \cot \alpha$ between folds (only when $\alpha > 45^\circ$). Figure 19 compares cylinders of $\alpha = 45^\circ$ and 54° .

$$\begin{aligned} x &= 2l + \frac{4m}{1 + \tan^2 \alpha \cos^2 \frac{\xi}{2}}, \\ y &= \frac{4m \tan \alpha \cos \frac{\xi}{2}}{1 + \tan^2 \alpha \cos^2 \frac{\xi}{2}}, \\ z &= \frac{\sin \frac{\xi}{2}}{\sin \frac{\xi_0}{2}} z_0. \end{aligned} \quad (5)$$

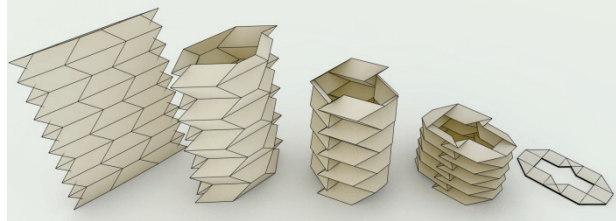


Figure 17. Cylinder of $\alpha = 45^\circ$ at $\beta = 89^\circ, 67.5^\circ, 45^\circ, 22.5^\circ$, and 1° (from left to right).

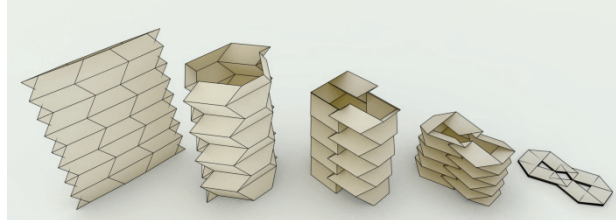


Figure 18. Cylinder of $\alpha = 54^\circ$ at $\beta = 89^\circ, 67.5^\circ, 45^\circ, 22.5^\circ$, and 1° (from left to right).

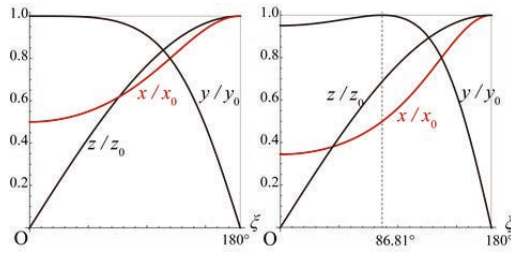


Figure 19. Folding motions of cylinders of $\alpha = 45^\circ$ (left) and 54° (right).

4.4 Cellular Structure

The example cylinder is composed of elements having translational symmetry to each other. Thus, the cylinder periodically tessellates the three-dimensional space without producing any gap, as shown in Figure 20. This tessellation property can be preserved for any folded state; hence, this tessellation has a synchronized one-DOF rigid-folding motion inherent from the cylinder. This volumetric polyhedral complex can smoothly fold itself into two flat states following the transformation of a single cylinder.

The general key technique for constructing a tessellatable rigid-foldable cylinder is to construct a module whose boundaries are translationally symmetric, such as the nine-panel module in Figure 13 and its compatible variation. Once we construct such a module, we can then apply symmetry operations (reflection and translation) based on the rhombus grid, as shown in Figure 21, to construct a valid cellular mechanism.

4.5 Generalization

In order to construct such a module, we use joint structures composed of four-valence bi-directionally flat-foldable vertices classified into fold and elbow types (Figure 22). Such a joint vertex converts the shared dihedral folding angle ξ to a sectional folding angle ϕ at each joint.

$$\phi_{\text{Fold}} = 2 \arctan \left(\cos \frac{\xi}{2} \tan \frac{\phi_0}{2} \right), \quad (6)$$

$$\phi_{\text{Elbow}} = 2 \operatorname{arccot} \left(\cos \frac{\xi}{2} \cot \frac{\phi_0}{2} \right).$$

Here, we aim to construct a one-DOF mechanism by connecting such joint mechanisms so that its ends are always parallel, i.e., $\sum \phi = 0$ or $\pm \pi$. Such a mechanism can be constructed by combining the following identity equations.

$$\begin{aligned} \phi_{\text{Fold}}(\phi_0, \xi) + \phi_{\text{Fold}}(-\phi_0, \xi) &\equiv 0, \\ \phi_{\text{Elbow}}(\phi_0, \xi) + \phi_{\text{Elbow}}(-\phi_0, \xi) &\equiv 0, \\ \phi_{\text{Fold}}(\phi_0, \xi) + \phi_{\text{Elbow}}(\pi - \phi_0, \xi) &\equiv \pi. \end{aligned} \quad (7)$$

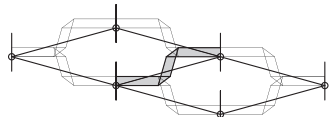


Figure 21. Pair of cylinders produced from one module (left) and repeated cylinders using a rhombus grid (right).

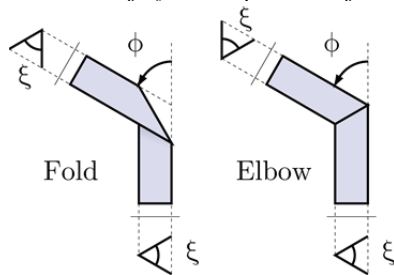


Figure 22. Fold and elbow.

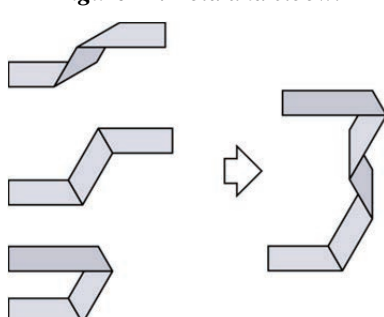


Figure 23. Combining vertices to form an angular identity equation.

The ordering of vertices does not alter the total angle; thus, we can easily construct compatible variations of valid half strips, an example of which is shown in Figure 23.

A cellular structure proposed by Hoberman [3] can be constructed using this sequence. Therefore, it is a bi-directionally flat-foldable type structure and thus a rigid-foldable structure.

Moreover, bi-directionally flat-foldable structures comprising planar quadrilateral panels can be further generalized into non-symmetric freeform designs by using sufficient conditions for rigid-foldability [12].

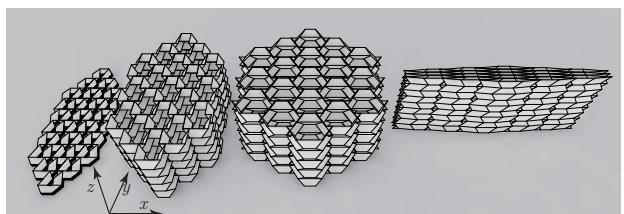
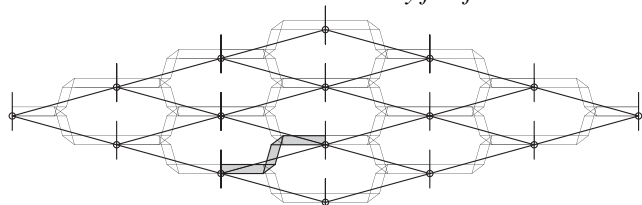


Figure 20. Tessellation of a cylinder to produce a one-DOF bi-directionally flat-foldable cellular structure.



5. WOVEN CYLINDER CELLS

5.1 Geometric Construction

In previous sections, we considered cellular structures whose component cylinders are all aligned in the z direction. In this section, we propose a novel cellular structure where the component cylinders are “woven” in the $y-z$ directions (Figure 24). The structure can be formed by the following procedure.

1. Align the cells side by side (in the y direction of Figure 4) to form a cellular layer (Figure 25). This compound layer comprises top and bottom corrugated surfaces, each of which is transformable: egg-box type parallelogram meshes. Here, note that the top and bottom surfaces are congruent to each other with a phase shift and essentially have fourfold symmetry.

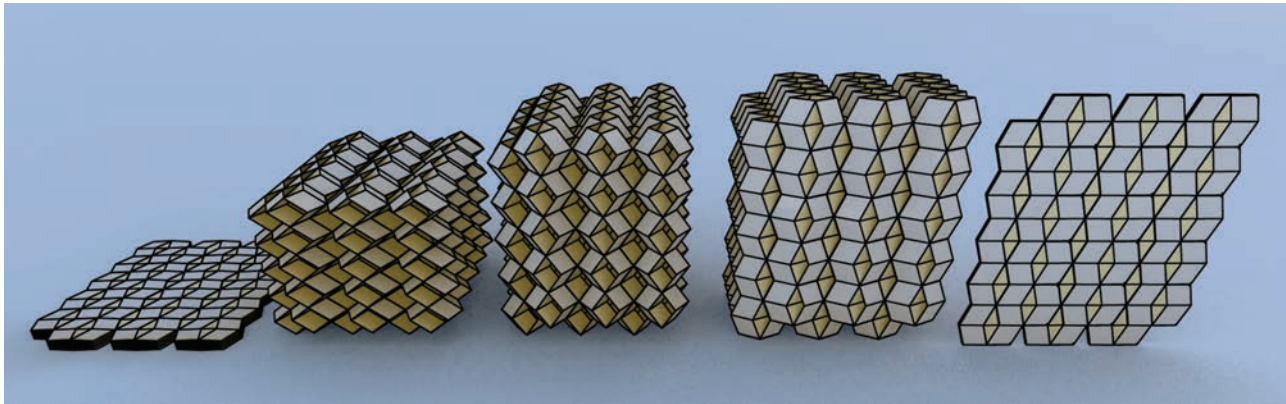


Figure 24. Woven-type cellular structure.

2. Stack the layers to tessellate a 3D space. Here, we have two choices for the orientation of each layer to be stacked because of the fourfold symmetry of the egg-box type mesh.
3. By alternating the orientation of the tubes for each layer, we get a “woven” type cellular structure (Figure 26 left). Note that if we always choose parallel layers, we obtain the basic cellular structure (Figure 26 right).

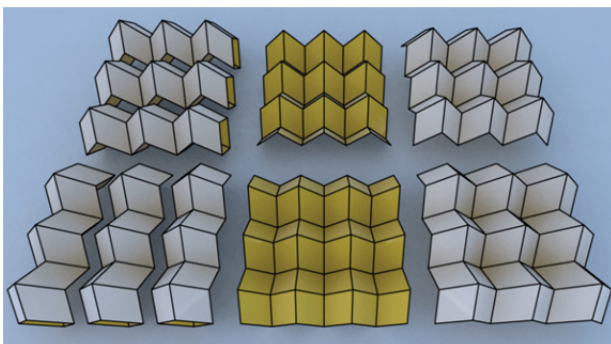


Figure 25. We can construct an egg-box surface by aligning cells side by side.

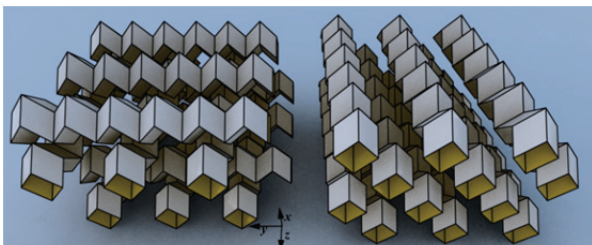


Figure 26. Woven structure (left) and basic cellular structure (right).

5.2 Kinetic Behavior

The motion of a woven cylinder assembly can be

understood by observing its smallest motif composed of two basic modules (two identical rhombic modules or a pair of modules with corresponding proportion) (Figures 27 and 28). This polyhedral shape is known in the origami field as *flip-flop*, a kinetic origami model (from one piece of rectangular paper) originally designed by Yenn [3]. The original flip-flop uses a 60° rhombus, but arbitrary parallelograms can form such a one-DOF mechanism. The convex hull of the flip-flop is a dodecahedron composed of parallelograms, which tessellates the 3D space without gaps in any folded state, in the way rhombic dodecahedra tessellate space. The whole woven cylinder structure is constructed with only translational copies of the module; thus, the transformation mode simply follows that of a flip-flop.

The x dimension of a flip-flop is the sum of the x dimensions of its two component modules (x and x'). These two modules are in opposite folding states, i.e., parameter ξ in one module is equal to parameter Ξ in another module or $x'(\xi) \equiv x(\Xi)$. Figure 29 shows the change in the x , y , and z dimensions of a flip-flop using a rhombus with $\theta_0 = 2 \arctan(\sqrt{2}/2)$, i.e., the silver rhombus.

A flip-flop—and thus a woven cylinder structure—always has the minimum x value in an intermediate folded state. This means that the structure stabilizes with x directional compression and is stiff in this direction. For $\theta_0 = 2 \arctan(\sqrt{2}/2)$, the structure stabilizes at the state where the module becomes a rhombic dodecahedron ($\xi = 120^\circ$ and $y = z$) that holds the maximum volume.

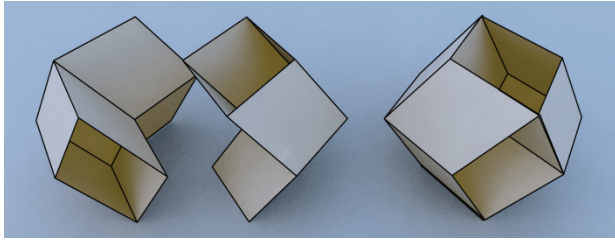


Figure 27. Construction of woven cylinder module: flip-flop by Yenn.

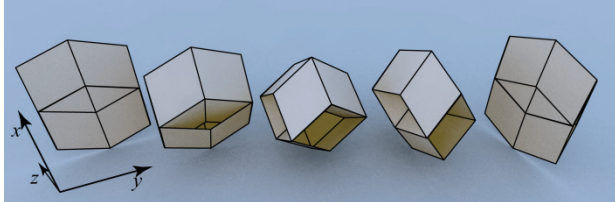


Figure 28. Folding motion of a flip-flop. Note the change in x (height). The middle state forms a rhombic dodecahedron.

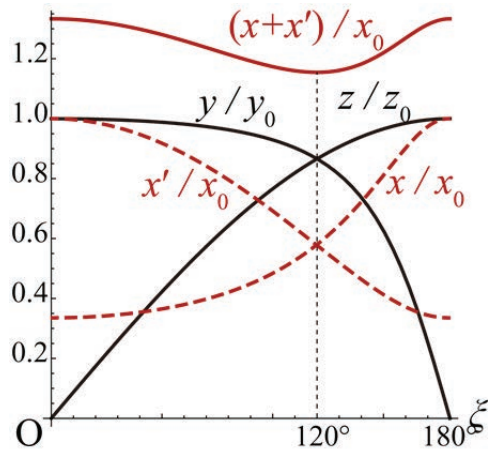


Figure 29. Change in the dimensions of a flip-flop or a woven cylinder cell (compare with Figure 6).

6. POTENTIAL APPLICATIONS

Since the cylindrical and cellular structures we have shown are purely geometric and thus free of scale, the field of potential application ranges from microstructures to architecture. Here, we suggest a few potential orientations, but the applications are open-ended.

By placing planes at the ends of a TMP-type cylinder, we can construct a closed and flexible polyhedron, i.e., bellows, holding a certain volume. By folding this bellows, we can observe that it continuously reduces its volume to zero. In theory, this type of transformable polyhedron does not exist

because it is against Connelly's bellows theorem. In reality, a small and local distortion at the ends of cylinders occurs with elastic material; the distortion is caused by constraining shear deformation of the boundaries.

Because the distortion is local, it seems plausible to use the bellows for practical purposes; one example is a fluid actuator. Figure 30 shows an illustrated image of the actuator. The actuator has a long stroke (close to 100% of its length) because it does not require a piston.

The applications of the cellular structures include collapsible temporary shelters constructed from stiff panels. The virtue of the cell structure in this context is that each cell acts as a volumetric building block that supports its self-weight and force while insulating sound and heat. For example, we can build thick walls that collapse to very thin states (Figure 32).

We can further interpret the cellular structures as anisotropic materials from a macroscopic viewpoint. In other words, we use the intersection between some given volumetric form and the fine cellular structure filling infinite 3D space (example shown in Figure 32). This intersection follows the same one-DOF transformation mechanism as the infinite tessellation because of the redundant geometric constraints that work in cylindrical and cellular structures.

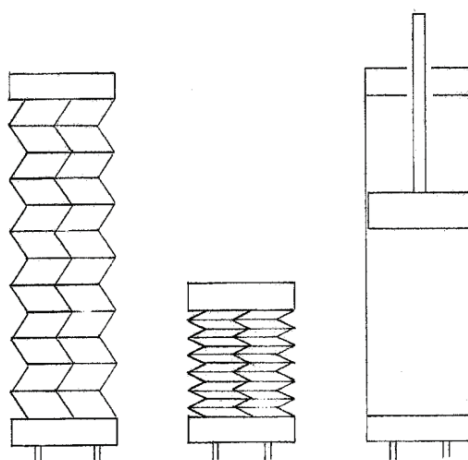


Figure 30. Actuator from rigid-foldable cylinder (left and middle) compared with a conventional actuator.

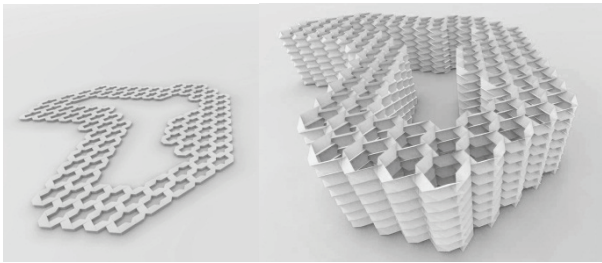


Figure 31. Assembly of collapsible building blocks.



Figure 32. Collapsible sphere from woven cylinders.

7. CONCLUSION

We introduced novel families of rigid-foldable cylinders and three types of cellular structures based on cylinders: i.e., zonogon extrusion cells, bi-directionally flat-foldable cells, and woven cylinder cells. We showed their geometric validity as one-DOF structures, their generalized design method, and their kinetic properties. We suggested the orientations of potential applications of these structures.

8. ACKNOWLEDGEMENTS

This study is supported by KAKENHI (22800009), a Grant-in-Aid for Research Activity Start-up by the Japan Society for the Promotion of Science. Further, this study is supported by the JST PRESTO program.

REFERENCES

- [1] **Hoberman, C.**, Curved pleated sheet structures, *United States Patent*, No. 5,234,727, 1993.
- [2] **Guest, S. D., and Pellegrino, S.**, The folding of triangulated cylinders, Part I: Geometric considerations, *ASME Journal of Applied Mechanics*, Vol. 61, 1994, pp. 773-777.
- [3] **Sogame, A., and Furuya, H.**, Conceptual study on cylindrical deployable space structures, *IUTAM-IASS Symposium on Deployable Structures: Theory and Applications*, 2000, pp. 383-392.
- [4] **Nojima, T.**, Origami modeling of functional structures based on organic patterns, Presentation Manuscript at VIPSI Tokyo, 2007.
- [5] **Kuribayashi, K., Tsuchiya, K., You, Z., Tomus, D., Umemoto, M., Ito, T., and Sasaki, M.**, Self-deployable origami stent grafts as a biomedical application of Ni-rich TiNi shape memory alloy foil, *Materials Science and Engineering A*, Vol. 419, 2006, pp. 131-137.
- [6] **Wu, Z., Hagiwara, I., and Tao, X.**, Optimisation of crush characteristics of the cylindrical origami structure, *International Journal of Vehicle Design*, Vol. 43, 2007, pp. 66-81.
- [7] **Miura, K.**, Proposition of pseudo-cylindrical concave polyhedral shells, *Proc. IASS Symposium on Folded Plates and Prismatic Structures*, 1970.
- [8] **Tachi, T.**, One-DOF cylindrical deployable structures with rigid quadrilateral panels, *Proc. IASS Symposium 2009*, Eds. Domingo, A., and Lazaro, C., 2009, pp. 2295-2306.
- [9] **Miura, K., and Tachi, T.**, Synthesis of rigid-foldable cylindrical polyhedra, *J. ISIS-Symmetry*, Special Issues for the Festival-Congress Gmuend, Austria, 2010, pp. 204-213.
- [10] **Hoberman, C.**, Reversibly expandable three-dimensional structure. *United States Patent*, No. 4,780,344, 1988.
- [11] **Yenn, T.**, *Flip-Flop*, <http://erikdemaine.org/thok/flipflop.html>
- [12] **Tachi, T.**, Freeform rigid-foldable structure using bidirectionally flat-foldable planar quadrilateral mesh, *Advances in Architectural Geometry 2010*, 2010, pp. 87-102.